# MiR-15b-5p Promotes Growth and Metastasis of Renal Clear Cell Carcinoma

## MiR-15b-5p Promueve el Crecimiento y la Metástasis del Carcinoma Renal de Células Claras

**Xing Bi; Mengzhen Tian & Peng Chen**

**SUMMARY:** We investigated the expression and clinical significance of miR-15b-5p in clear cell renal cell carcinoma (RCC) through bioinformatics analysis and experimental verification. The differentially expressed miRNAs were screened in the GEO database. Venn diagram showed that there were 5 up-regulated miRNAs (has-miR-210, has-miR-142-3p, has-miR-142-5p, has-miR-15b-5p, and has-miR-193a-3p) and only 1 down-regulated miRNA (has-miR-532-3p) that were commonly expressed between GSE189331 and GSE16441 datasets. This was further confirmed in TCGA. Further analysis showed that the has-miR-193a-3p, has-miR-142-3p, has-miR-142-5p, and has-miR-15b-5p were closely related to tumor invasion, distant metastasis and survival probability. The expression of miR-15b-5p in ccRCC tissues was significantly higher than that in adjacent normal kidney tissues (P<0.05). The expression of miR-15b-5p had no significant relationship with gender, age, smoking history, body mass index, T stage and pathological nuclear grade (P>0.05). Following inhibition of miR-15b-5p expression, RCC cells had attenuated proliferation, increased apoptosis, and attenuated migration and invasion. has-miR-15b-5p-WEE1, has-miR-15b-5p-EIF4E, has-miR-15b-5p-PPP2R1B may be three potential regulatory pathways in ccRCC. miR-15b-5p is highly expressed in cancer tissues of ccRCC patients. It may promote proliferation, inhibit apoptosis and enhance cell migration and invasion of RCC cells. The has-miR-15b-5p-WEE1, has-miR-15b-5p-EIF4E, and has-miR-15b-5p-PPP2R1B may be three potential regulatory pathways in ccRCC.

**KEY WORDS: MicroRNA; Clear cell renal cell carcinoma; Real-time PCR; Spread; Migration; Bioinformatics analysis.**

## INTRODUCTION

Renal cell carcinoma (RCC) accounts for about 3 % of adult malignancies, and its incidence has been on the rise in recent years (Ferlay *et al.*, 2018). Clear cell renal cell carcinoma (ccRCC) is the most common subtype of RCC, accounting for 75 %-80 % (Moch *et al.*, 2016). With the development and popularization of imaging technology, the detection rate of early ccRCC has increased (Bai *et al.*, 2015). Surgery is the most effective treatment for early ccRCC (Spyropoulou *et al.*, 2021). Nonetheless, approximately 17 % of ccRCC patients have distant metastases at diagnosis, and nearly 30 % to 40 % still develop metastases after radical resection (Skolarikos *et al.*, 2007). At present, the treatment mode of metastatic ccRCC has changed from targeted therapy and immunotherapy to immune combination therapy (Motzer *et al.*, 2019). Even so, the 5-year survival rate of ccRCC patients is only 26 %-43 % (Albiges *et al.*, 2020; Motzer *et al.*, 2020). Therefore, the treatment of ccRCC needs to be further improved.

MicroRNAs (miRNAs) are single-stranded non-protein-coding RNAs with average length of 18-26 nt. They play important roles in tumor cell development, apoptosis, invasion, etc. (Calin *et al.*, 2004; Medina & Slack, 2008). Among them, miR-15b-5p is abnormally expressed in liver cancer, colorectal cancer, and glioma, and may affect the occurrence and development of tumors (Pang *et al.*, 2015; Zhang *et al.*, 2015; Li *et al.*, 2016a). MiRNAs, including miR-15b-5p, are also involved in ccRCC (Osanto *et al.*, 2012; Ishihara *et al.*, 2014). Previous studies have mainly focused on the differential expression of miR-15b-5p in ccRCC cancer tissue and normal kidney tissue and its significance for diagnosis and prognosis. However, the specific mechanism of miR-15b-5p in ccRCC is rarely studied.

Herein, we investigated the expression difference of miR-15b-5p in ccRCC and adjacent normal kidney tissue, and analyzed its clinical significance in ccRCC. The

Department of Urology, Affiliated Tumor Hospital of Xinjiang Medical University, Urumqi, P.R. China.

biological function of miR-15b-5p in ccRCC was analyzed at the cellular level, and its possible underlying mechanism was further studied by bioinformatics analysis. Our findings may provide new methods for the prognosis and treatment of ccRCC.

## MATERIAL AND METHOD

**Identification of differentially expressed miRNAs in ccRCC.** GSE16441 and GSE189331 datasets were obtained from the GEO (Gene Expression Omnibus database) database (http://www.ncbi.nlm.nih.govgeo). GSE16441 dataset contains 17 cases of normal tissues and 17 cases of ccRCC tissues; while, GSE189331 dataset contains 5 normal tissues and 6 ccRCC tissues. GEO2R in the GEO database (http://www.ncbi.nlm.nih.gov/geo/geo2r) was used to screen the differentially expressed miRNAs, which were visualized using volcano plots and cluster heatmaps. The screening criteria were |log2(fold change)|>1.5 and p-value<0.05. The common differentially expressed miRNAs between GSE16441 and GSE189331 datasets were analyzed with Venn diagram (http://bioinformatics.psb.ugent.be/webtools/Venn/) and then their levels were further verified in GSE16441dataset, GSE189331 dataset and, TCGA database ( https://portal.gdc.cancer.gov/). R language was used for statistical analysis and visualization.

**Effect of common differentially expressed miRNAs on overall survival (OS).** Survival analysis (Kaplan-Meier method) of differential genes was performed using R language.

**Relationship of common differentially expressed miRNAs with T stage, M stage and N stage of ccRCC.** The relationship of common differentially expressed miRNAs with T stage, M stage and N stage of ccRCC was analyzed in the TCGA (https://portal.gdc.cancer.gov/) database. Statistical analysis and visualization were performed by R language.

**Target mRNA of miR-15b-5p and enrichment analysis.** The miRDB (http://mirdb.org/), miRWalk (http://mirwalk.umm.uni-heidelberg.de/) and TargetScan databases (https://www.targetscan.org/) were used to predict the target mRNAs of miR-15b-5p. To determine the biological functions of miR-15b-5p target mRNAs, we performed GO and KEGG pathway enrichment analysis with R software.

**Construction of protein-protein interaction (PPI) network.** We used STRING (http://stringdb.org/) to construct the PPI network of miR-15b-5p target mRNAs. The PPI network was visualized using Cytoscape version 3.9.1. The nodes of PPI network were sorted according to

the degrees. The top 10 hub genes of miR-15b-5p in PPI network were screened. The expression levels of top 4 hub genes of miR-15b-5p in PPI network were validated in TCGA database. Statistical analysis and visualization were performed by R language.

**Specimen collection.** Totally, 27 pairs of surgically resected fresh cancerous tissues and adjacent normal kidney tissues were collected from ccRCC patients (n=27). These 27 ccRCC patients were admitted from April, 2011 to January, 2018. They received radical or partial nephrectomy. Other benign nephrotic lesions were excluded, and no tumor-related treatment was performed before surgery. The basic clinical data of these patients are shown in Table I. All specimens were confirmed by pathologists according to the 2016 WHO classification criteria. The cells were graded using the WHO/ISUP four-stage grading system, and the staging was determined with the TNM staging system 2017 VERSION. This study was approved by the Ethics Committee of Cancer Hospital Affiliated to Xinjiang Medical University. Written informed consent was obtained from patients.

Table I. Basic clinical data of patients and miR-15b expression.

| | N | Mean ± standard deviation | t | P |
|---|---|---|---|---|
| Sex | | | 0.72 | 0.48 |
| Male | 18 | 1.52±0.93 | | |
| Female | 9 | 1.82±1.17 | | |
| Age (years) | | | -0.914 | 0.38 |
| ≥50 | 19 | 1.48±0.79 | | |
| <50 | 8 | 1.96±1.39 | | |
| Smoking | | | -0.146 | 0.89 |
| Yes | 10 | 1.58±1.15 | | |
| No | 17 | 1.64±0.95 | | |
| Body mass index (kg/m²) | | | -1.65 | 0.14 |
| ≥25 | 20 | 1.38±0.69 | | |
| <25 | 7 | 2.31±1.45 | | |
| T Stage | | | 2.06 | 0.05 |
| T1~T2 | 18 | 1.35±0.86 | | |
| T3~T4 | 9 | 2.15±1.12 | | |
| Nuclear classification (WHO classification) | | | 0.92 | 0.37 |
| G1~G2 | 20 | 1.51±0.92 | | |
| G3~G4 | 7 | 1.92±1.25 | | |

**Real-time PCR.** Total RNAs were extracted from tissue samples or cells using the Trizol method and reverse transcribed into cDNA. The primer sequence for miR-15b-

5p was as follows: 5'-GCAGTAGCAGCACATCA-3'. The PCR reaction volume was 10 µL, including 0.7 µL of miR-15b-5p forward and reverse primers, 5 µL of 2×SYBR Green Select Mix, 1 mL of cDNA template, and 0.05 µL of ROX. The reaction conditions were: pre-denaturation at 95 °C for 2 min, and 40 cycles of denaturation at 95 °C for 20 s, and annealing at 60 °C for 30 s. U6 snRNA was used as an internal control. The relative expression of miR-15b-5p was calculated using $2^{-\Delta\Delta Ct}$ method.

**Cell line and treatment.** Caki-1 RCC cells were derived from Procell (Wuhan, China). They were cultured in McCoy's 5A medium supplemented with 10 % fetal bovine serum and 1 % Penicillin-Streptomycin at 37 °C, 5 % CO2. According to different treatments, cells were divided into blank control group, inhibitor control group, and miR-15b-5p-inhibitor group. Cells in blank control group were cultured normally without any treatment. Cells in inhibitor control group and miR-15b-5p-inhibitor group were treated with inhibitor negative control (0.1 mM; GenePharma, Shanghai, China) and miR-15b-5p-inhibitor (0.1 µM; GenePharma), respectively. The treatment lasted for 48 h.

**CCK-8 assay.** Caki-1 cells were seeded into a 96-well plate (100 µL/well, $5 \times 10^3$ cells/well) and cultured for 24 h. The treatment with miR-15b-5p inhibitor was carried out as above described. After 48 h, 100 µL of the prepared 10 % CCK-8 solution was added. After incubation for 1 h, the OD value at 450 nm was measured with a microplate reader (xMark™; Bio-Rad).

**Cell apoptosis analysis.** After treatment with miR-15b-5p inhibitor for 48 h, cells were collected, fixed, and re-suspended in 500 µL 1×Binding Buffer. Then, cells were incubated with 5 µL Annexin V-PE and 10 µL 7-AAD (BD; cat# 559763) at 4°C for 10 min in the dark. After that, cells were analyzed on a flow cytometer (LSRFortessa; BD).

**Transwell assay.** Cells were collected and re-suspended in serum-free medium after treatment with miR-15b-5p inhibitor for 48 h. Then, 100 µl of cell suspension was added to the upper chamber coated without (for cell migration analysis) or with Matrigel (for cell invasion analysis). The 600 µl of complete medium was added to the lower chamber. Three duplicate wells were set in each group. After incubation for 72 h, the upper chamber was removed and fixed with 4 % formaldehyde at room temperature for 20 min. Then, the upper chamber was successively stained with 400 µl of Giemsa stain solution A at room temperature for 1 min and 800 µl of Giemsa stain solution B at room temperature for 5 min. After staining, cells were observed under microscope. The invaded and migrated cells were counted.

**Statistical analysis.** Statistical analysis was performed using SPSS 26.0 statistical software. Paired t-test was used to analyze the expression differences of miR-15b-5p in renal clear cell carcinoma tissues and adjacent normal kidney tissues. Associations between miR-15b-5p expression levels and clinicopathological features were performed using two independent samples t-tests. ROC was used to evaluate the ability of miR-15b-5p to diagnose ccRCC, and the optimal cut-off value of miR-15b-5p as a diagnostic marker was obtained. According to the optimal cutoff value, the expression of miR-15b-5p in ccRCC tissues was divided into high expression and low expression. The Kaplan-Meier method and Cox multivariate analysis was used to analyze the relationship between miR-15b-5p expression and disease-free survival (DFS). All experimental data are expressed as mean ± standard deviation. One-way ANOVA was used for multiple comparisons among groups. $P<0.05$ was considered statistically significant.

## RESULTS

**Differentially expressed miRNAs.** In the GSE189331 dataset, there were a total of 93 miRNAs differentially expressed between normal tissues and tumor tissues, including 46 up-regulated miRNAs and 47 down-regulated miRNAs. The volcano plot of differentially expressed miRNAs in GSE189331 dataset was shown in Figure 1A. The heatmap of the top 40 differentially expressed miRNAs was shown in Figure 1B. In the GSE16441 dataset, 40 differentially expressed miRNAs were identified between normal tissues and tumor tissues, including 9 up-regulated genes and 31 down-regulated genes. Volcano plot displayed the differentially expressed miRNAs in GSE16441 dataset (Fig. 1C), while the heatmap showed the top 40 differentially expressed miRNAs (Fig. 1D).

Venn diagram showed that there were 5 up-regulated miRNAs (has-miR-210, has-miR-142-3p, has-miR-142-5p, has-miR-15b-5p, and has-miR-193a-3p) that were commonly expressed between GSE189331 dataset and GSE16441 data set (Fig. 2A). For the down-regulated miRNAs, only 1 miRNA (has-miR-532-3p) was commonly expressed between GSE189331 dataset and GSE16441 data set (Fig. 2B). A heatmap of the common differential miRNAs was also shown (Fig. 2C).

**Validation of the common differential miRNAs in GSE189331, GSE16441 and TCGA.** The expressions of the common differential miRNAs were further verified in GSE189331, GSE16441 and TCGA. As shown in Figures 3A-3L, 5 miRNAs of has-miR-210, has-miR-142-3p, has-
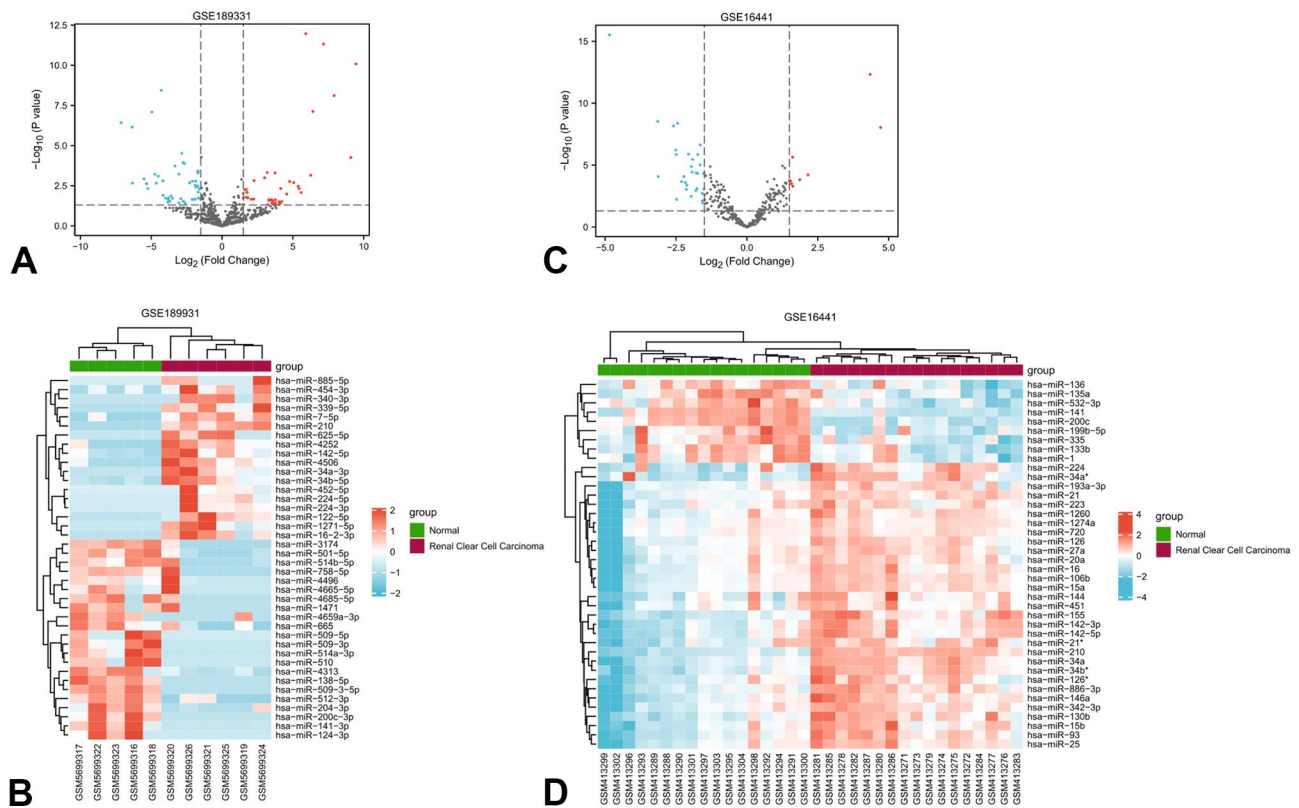
Fig. 1. Differential miRNAs in ccRCC. A: Volcano plot of differential miRNAs in GSE189331 dataset; B: Cluster heatmap of differential miRNAs in GSE189331 dataset; C: Volcano plot of differential miRNAs in GSE16441 dataset; D: Cluster heatmap of differential miRNAs in GSE16441 dataset.

miR-142-5p, has-miR-15b-5p, and has-miR-193a-3p were significantly up-regulated in tumor tissues than in normal tissues of GSE189331 and GSE16441 datasets (P<0.05). However, has-miR-532-3p was significantly decreased in tumor tissues (P<0.05).

Similarly, in the TCGA data base, the levels of has-miR-210, has-miR-142-3p, has-miR-142-5p, has-miR-15b-5p, and has-miR-193a-3p were significantly higher in tumor tissues, while has-miR-532-3p was significantly lower in tumor tissues, than normal tissues (P<0.05) (Figs. 4A and 4B).
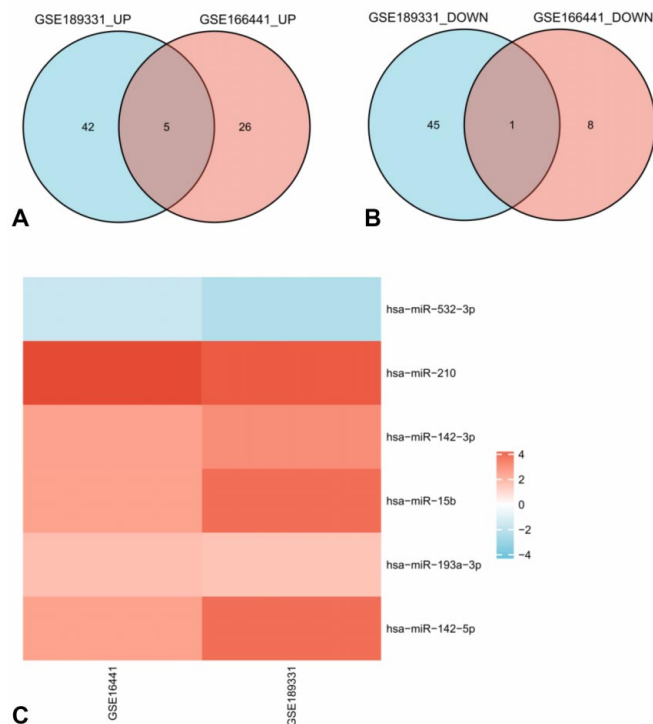


Fig. 2. Identification of common differential miRNAs. A: Venn diagram of up-regulated miRNAs in GSE189331 dataset and GSE16441 dataset. B: Venn diagram of down-regulated miRNAs in GSE189331 dataset and GSE16441 dataset. C: Heatmap of log fold change (FC) of common differential miRNAs. Up-regulated miRNAs are shown in red, while down-regulated miRNAs are shown in blue.
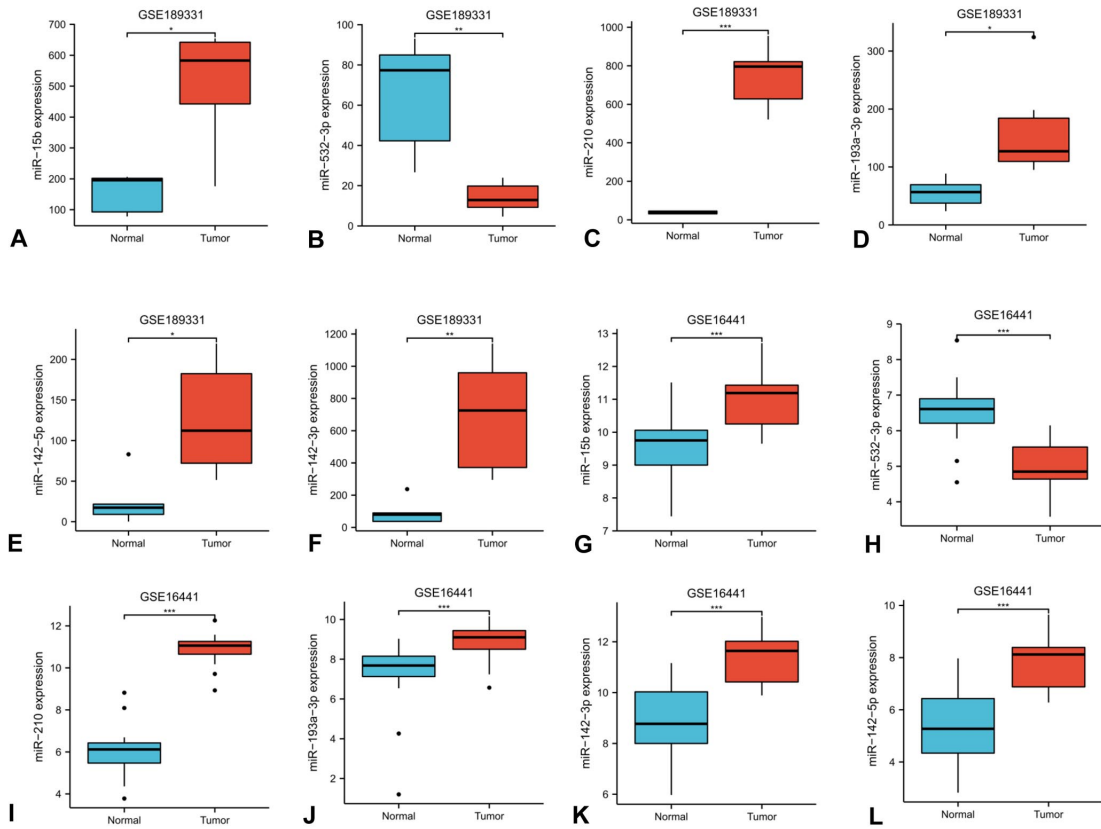
Fig. 3. Expression verification of common differential miRNAs in GSE189331 and GSE16441. A-F: The expression of common differential miRNAs in the GSE189331 dataset; G-L: The expression of common differential miRNAs in the GSE16441 dataset. *P<0.05, **P<0.01, ***P<0.001.
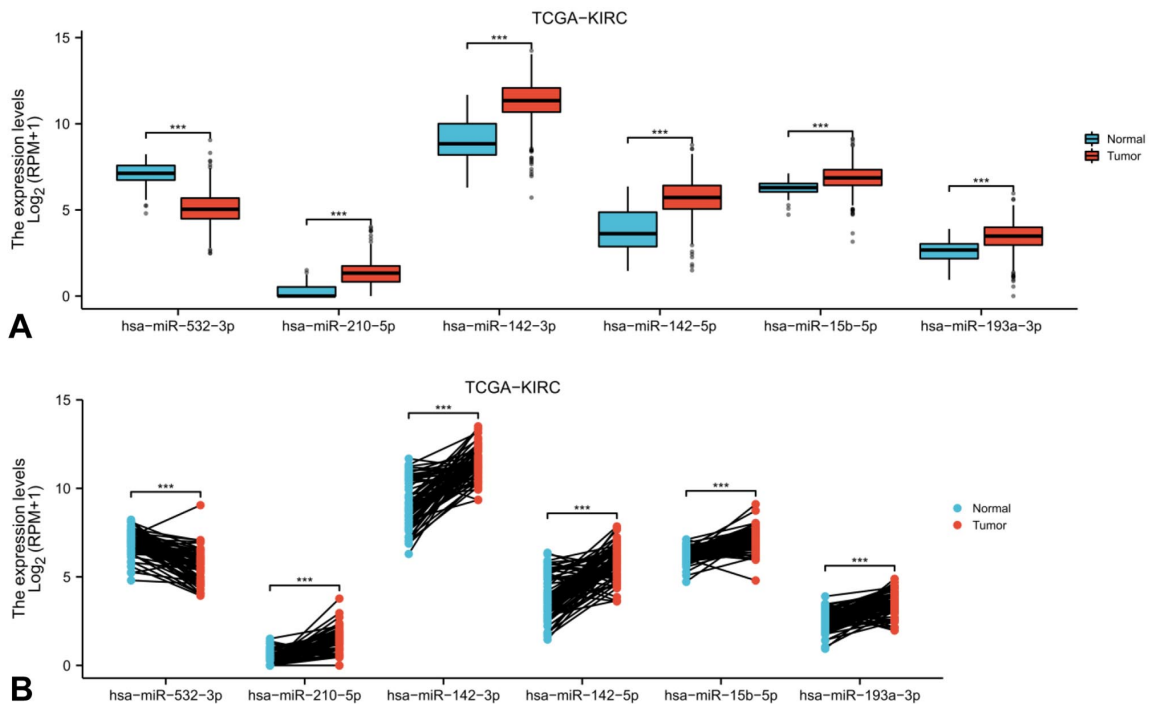


Fig. 4. Expression of common differential miRNAs in TCGA. A and B: The expression of common differential miRNAs in tumor tissue and normal tissue of TCGA. ***P<0.001.

**Effect of common differential miRNAs on OS.** To further understand whether these common differential miRNAs are potential prognostic markers for ccRCC, we analyzed the OS of patients. Among the six common differential miRNAs, the has-miR-193a-3p (Fig. 5A), has-miR-142-3p (Fig. 5C), has-miR-142-5p (Fig. 5D), and has-miR-15b-5p (Fig. 5E) were found to be associated with patient prognosis. Their high expression was significantly associated with poor OS of patients (P<0.05). However, the expression of has-miR-210-5p (Fig. 5B) and has-miR-532-3p (Fig. 5F) did not significantly affect OS of patients (P>0.05).

**Relationship of common differentially expressed miRNAs with T stage, M stage and N stage of ccRCC.** As shown in Figure 6A, the expression of has-miR-532-3p in T3 and T4 ccRCC tissues was lower than that in T1 and T2 (P<0.05), while the levels of has-miR-193a-3p, has-miR-142-3p, has-miR-142-5p and has-miR-15b-5p in T3 and T4 ccRCC tissues were higher than those in T1 and T2 (P<0.05). There was no significant difference in has-miR-210-5p. As shown in Figure 6B, the expression of hsa-miR-532-3p in N1 phase

ccRCC tissues was lower than that in N0 phase; whereas, hsa-miR-193a-3p expression in N1 phase ccRCC tissues was higher than that in N0 phase. No significant difference was found in has-miR-210-5p, has-miR-142-3p, has-miR-142-5p, and has-miR-15b-5p. Additionally, the expression levels of has-miR-193a-3p, has-miR-142-3p, has-miR-142-5p, and has-miR-15b-5p in M1 stage ccRCC tissues were significantly higher than those in M0 stage; while, the expressions of has-miR-210-5p and has-miR-532-3p were not significantly different (Fig. 6C). Thus, the has-miR-193a-3p, has-miR-142-3p, has-miR-142-5p, and has-miR-15b-5p were closely related to tumor local invasion (T stage) and distant metastasis (M stage).

**has-miR-15b-5p target gene prediction and GO/KEGG analysis.** The mechanism of has-miR-15b-5p in ccRCC is less studied. Therefore, in this study, has-miR-15b-5p was further studied. The downstream targets of has-miR-15b-5p were predicted using the miRDB, miRWalk and TargetScan databases. There were 172 common targets of has-miR-15b-5p in 3 databases (Fig. 7A). In addition, these 172 target
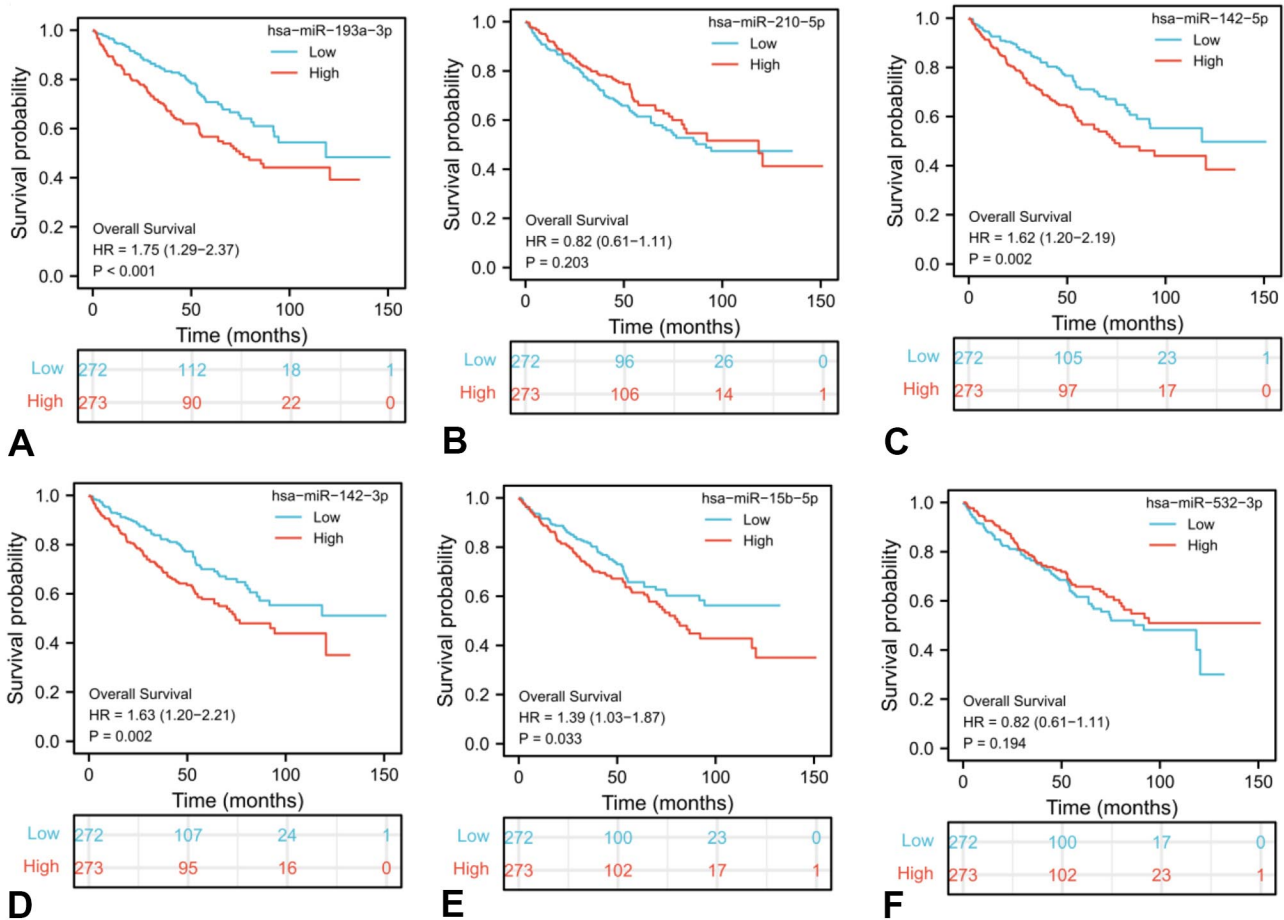


Fig. 5. Effect of common differential miRNAs on OS of ccRCC patients. The relationship of has-miR-193a-3p (A), has-miR-210-5p (B), has-miR-142-5p (C), has-miR-142-3p (D), has-miR-15b-5p (E), and has-miR-532-3p (F) with OS of ccRCC patients was analyzed.

genes were also subjected to GO and KEGG pathway enrichment analysis (Figs. 7B and 7C). GO analysis indicated that the has-miR-15b-5p target genes were involved in the protein polyubiquitination, protein kinase complex, and ubiquitin-like protein transferase activity (Fig. 7B). KEGG enrichment showed that the has-miR-15b-5p target genes were involved in P53 Progesterone-mediated oocyte maturation and other pathways (Fig. 7C).
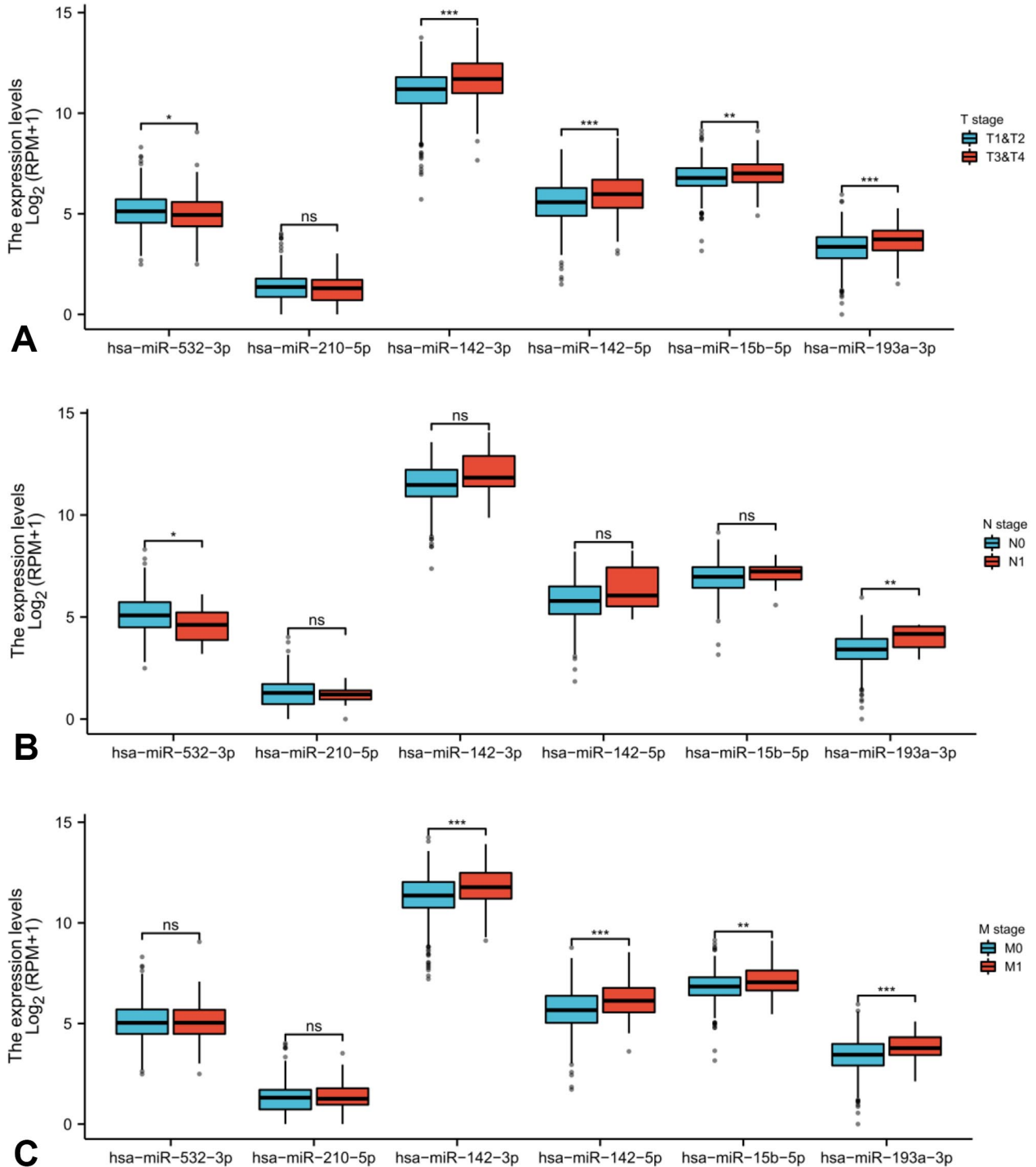


Fig. 6. Clinical significance of common differential miRNAs in ccRCC patients. The associations of common differential miRNAs with T stage (A), N stage (B), and M stage (C) of ccRCC were shown, respectively. *P<0.05, **P<0.01, ***P<0.001. ns, not significant.
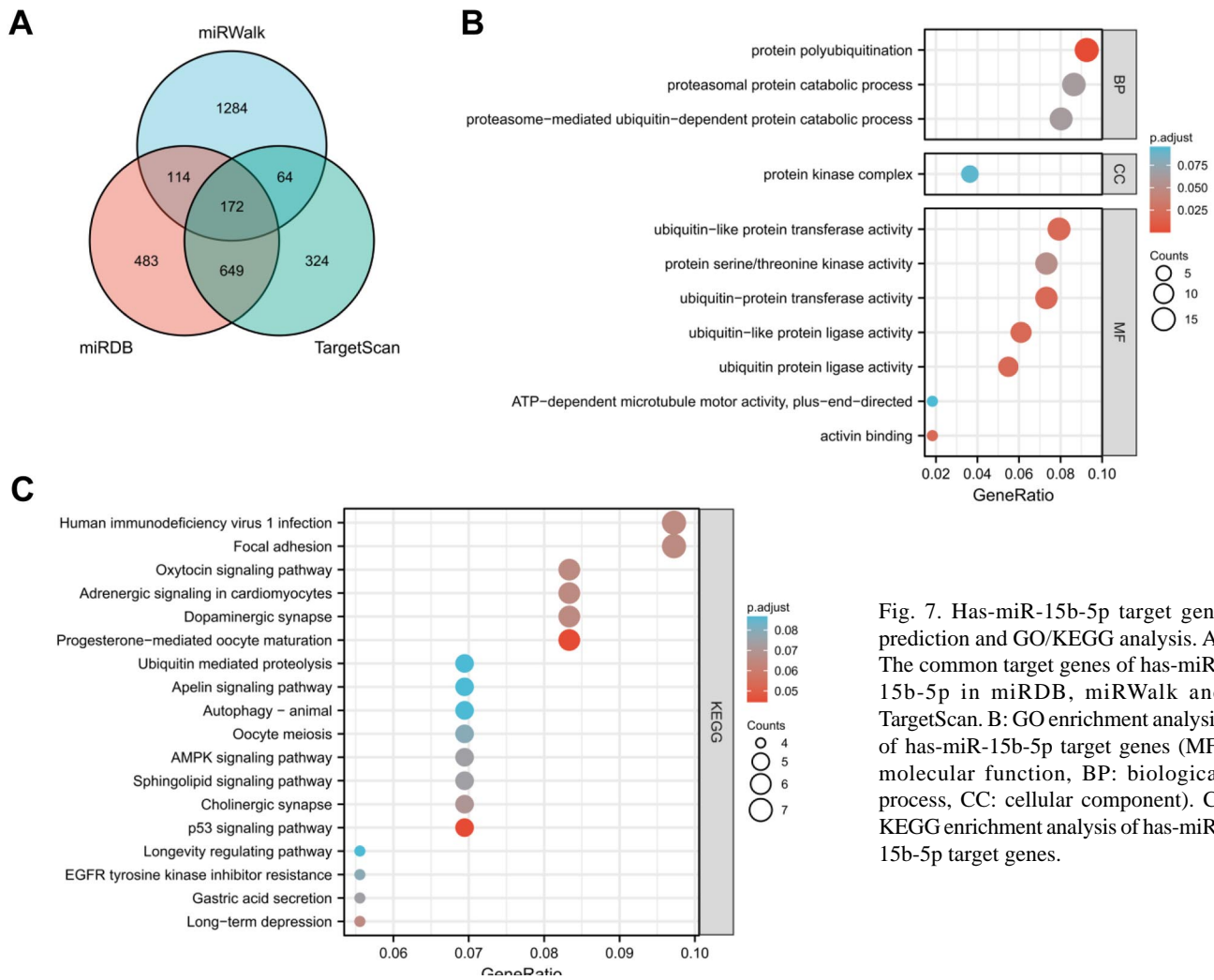
Fig. 7. Has-miR-15b-5p target gene prediction and GO/KEGG analysis. A: The common target genes of has-miR-15b-5p in miRDB, miRWalk and TargetScan. B: GO enrichment analysis of has-miR-15b-5p target genes (MF: molecular function, BP: biological process, CC: cellular component). C: KEGG enrichment analysis of has-miR-15b-5p target genes.

**PPI network.** The PPI network of miR-15b-5p target mRNAs was constructed with STRING and visualized with Cytoscape (Fig. 8A). According to the degree of each node, the top 10 hub genes included SMURF1 (SMAD-specific E3 ubiquitin protein ligase 1), EIF4E (eukaryotic translation initiation factor 4E), PPP2R1B (protein phosphatase 2 scaffold subunit A beta), WEE1 (WEE1 G2 checkpoint kinase), AKT3 (AKT serine/threonine kinase 3), GNAQ (G protein subunit a Q), IGF1R (insulin-like growth factor 1 receptor), USP14 (ubiquitin-specific peptidase 14), YOD1 (deubiquitinating enzyme), and, SIAH1 (siah E3 ubiquitin protein ligase 1) (Fig. 8B).

**Validation of has-miR-15b-5p target genes.** The expression levels of the top 4 hub genes (SMURF1, WEE1, EIF4E, and PPP2R1B) of has-miR-15b-5p in tumor and normal tissues were validated in the TCGA database. The results showed that SMURF1 in tumor tissue was significantly higher than that in normal tissue, while WEE1, EIF4E, and PPP2R1B in tumor tissue were significantly lower than those in normal tissue (P<0.05) (Fig. 9A). Additionally, WEE1, EIF4E, and PPP2R1B, but not SMURF1, were significantly associated with the OS of patients (Fig. 9B-9E). Therefore, has-miR-15b-5p-WEE1, has-miR-15b-5p-EIF4E, and has-miR-15b-5p-PPP2R1B may be three potential regulatory pathways in ccRCC.

**Experimental results**

*Expression of miR-15b-5p in ccRCC tumor tissue and adjacent normal kidney tissue.* Real-time PCR revealed that the expression level of miR-15b-5p in ccRCC cancer tissue was significantly higher than in adjacent normal kidney tissue (P=0.025) (Fig. 10A).

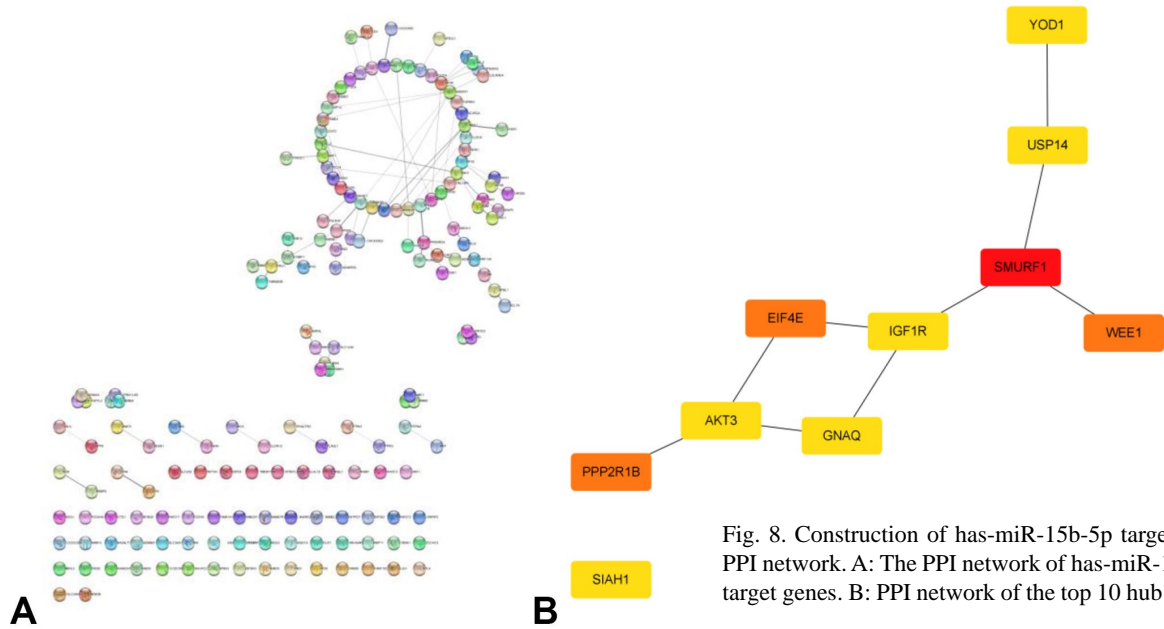Fig. 8. Construction of has-miR-15b-5p target gene PPI network. A: The PPI network of has-miR-15b-5p target genes. B: PPI network of the top 10 hub genes.
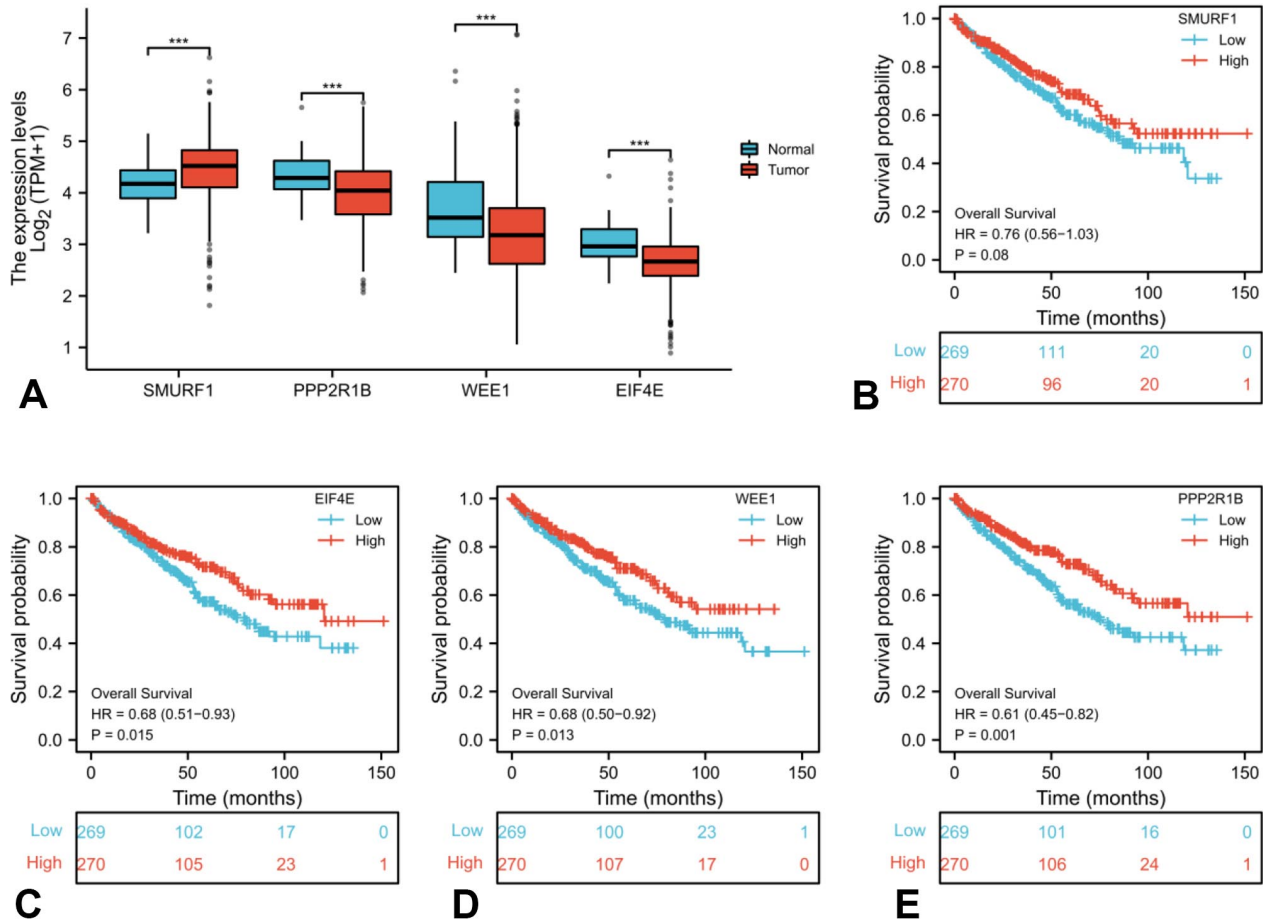


Fig. 9. Validation and prognostic role of has-miR-15b-5p target genes. A: Expression differences of SMURF1, WEE1, EIF4E, and PPP2R1B in tumor and normal tissues. B-E: Relationship of WEE1, EIF4E, and PPP2R1B with OS of patients. ***$P<0.001$.
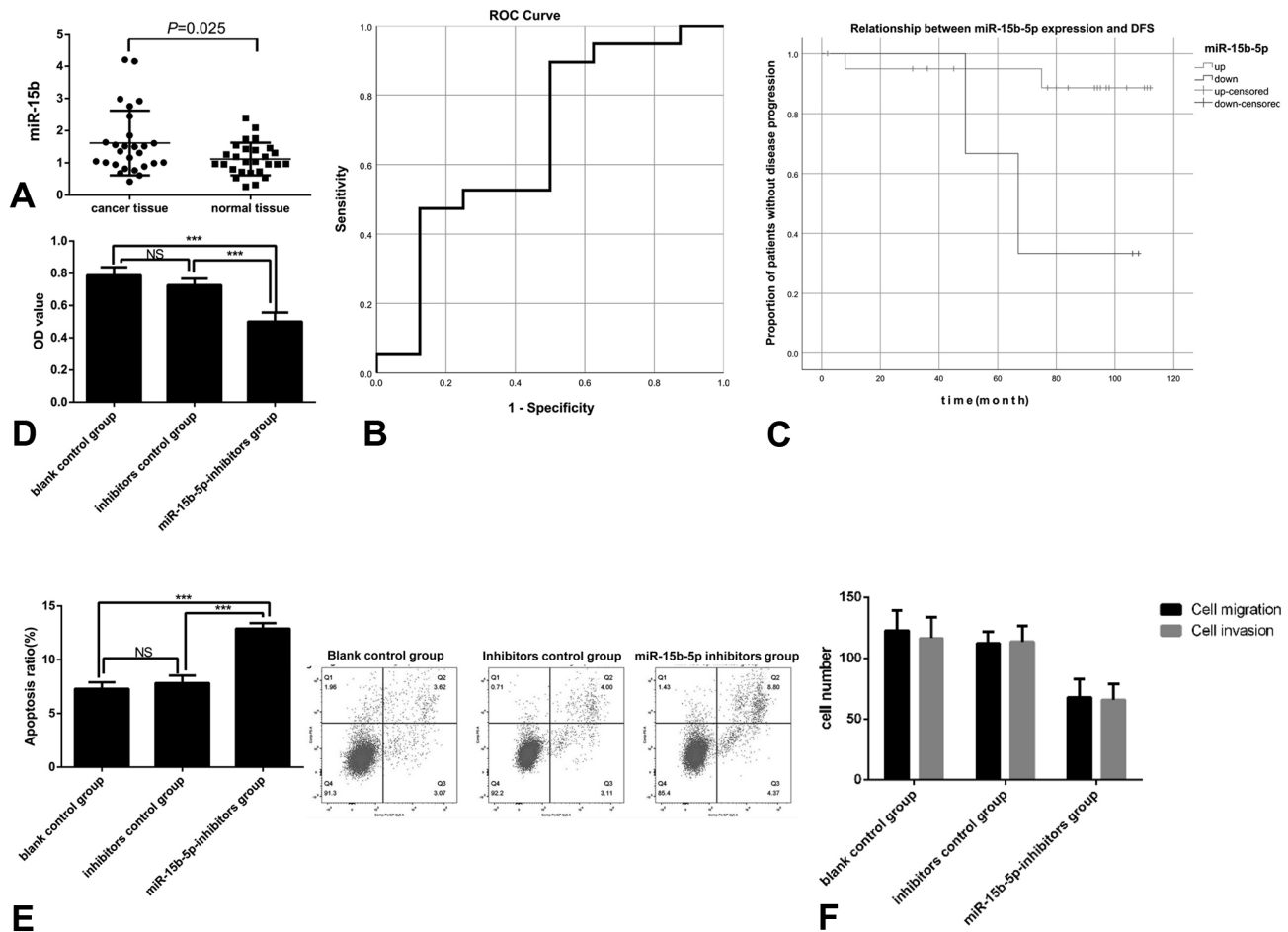
Fig. 10. Experimental results. A: Real-time PCR analysis of miR-15b expression in tumor tissues and adjacent normal kidney tissues. B: ROC analysis of miR-15b-5p to determine cut-off value. C: Survival curve. D: CCK-8 assay detected cell proliferation after treatment with miR-15b inhibitors. E: Flow cytometry analyzed cell apoptosis after treatment with miR-15b inhibitors. F: Transwell assay detected cell migration and invasion after treatment with miR-15b inhibitors. ***P<0.001. ns, not significant.

*The relationship between miR-15b-5p and clinicopathological features of ccRCC.* The expression level of miR-15b-5p in clear cell renal cell carcinoma was not significantly related with gender, age, smoking history, body mass index, T stage, and pathological nuclear grade (P>0.05) (Table I).

ROC curves were plotted based on the expression level of miR-15b-5p and the disease progression of the patients (Fig. 10B). The cutoff value of miR-15b-5p was determined at 0.9212. Kaplan-Meier survival analysis (Log-rank) showed that within 50 months, patients with high miR-15b-5p expression had shorter DFS. However, after 50 months, patients with high miR-15b-5p expression had longer DFS (Fig. 10C). COX multivariate analysis was performed. After adjusting age, gender, smoking history, T stage and nuclear grade, it was found that miR-15b-5p up-regulation was not a risk factor for disease progression in patients (P>0.05).

*Effect of miR-15b-5p on proliferation of Caki-1 cells.* CCK-8 assay showed that the OD values of blank control group and inhibitor control group were not significantly different (0.788±0.050 vs 0.726±0.041, P>0.05). However, the OD value of miR-15b-5p-inhibitor group was 0.500±0.057, which was significantly lower than that of blank control group and inhibitor control group (P<0.05) (Fig. 10D), indicating that miR-15b-5p may promote cell proliferation.

*Effect of miR-15b-5p on apoptosis of Caki-1 cells.* The apoptosis was detected with flow cytometry. As shown in Figure 10E, there was no significant difference in apoptosis rate between the inhibitor control group and blank control group (7.290±0.616 vs 7.827±0.701; P>0.05). The apoptosis rate of miR-15b-5p-inhibitors group was 12.897±0.508, which was significantly higher than that of blank control group and inhibitor control group (P<0.05). This indicates that miR-15b-5p may suppress cell apoptosis.

*Effect of miR-15b-5p on migration and invasion of Caki-1 cells.* Cell migration and invasion were assessed with Transwell assay. The number of migrated cells in the blank control group and inhibitor control group was 122.778±16.476 and 112.000±9.695, respectively, without significant difference (P>0.05) (Fig. 10F). Similarly, the number of invaded cells in the blank control group was 116.444±17.155, which was not significantly different from that in the inhibitor control group (113.556±12.914) (P>0.05) (Fig. 10F). However, the number of migrated and invaded cells in the miR-15b-5p inhibitor group was 68.000±14.714 and 65.778±13.160, significantly lower than that of the blank control group and the inhibitor control group (P<0.05). Thus, miR-15b-5p may promote cell migration and invasion.

## DISCUSSION

In this study, by using bioinformatics analysis, we found that there were high expression levels of has-miR-210, has-miR-193a-3p, has-miR-142-3p, has-miR-142-5p, and has-miR-15b-5p, but low level of has-miR-532-3p in ccRCC. However, only has-miR-193a-3p, has-miR-142-3p, has-miR-142-5p, and has-miR-15b-5p were associated with poor OS of patients and with tumor invasion and distant metastasis. Studies have shown that has-miR-193a-3p is lowly expressed in various tumors and inhibits the proliferation of tumor cells (Wang *et al.*, 2020; Wen *et al.*, 2021). Liu *et al.* (2018) found that miR-199a-3p was lowly expressed in ccRCC and played a tumor suppressor role. However, other studies (Liu *et al.*, 2017; Bao *et al.*, 2022) showed that, unlike other tumors, has-miR-193a-3p is often highly expressed in ccRCC, and promotes the proliferation and metastasis of ccRCC by regulating the PTEN pathway. Consistently, in this study, we found that has-miR-193a-3p was highly expressed in ccRCC and was related to tumor invasion. The difference in the expression and role of has-miR-193a-3p in ccRCC may be caused by different sample numbers or cell lines. Therefore, the expression, role and mechanism of has-miR-193a-3p in ccRCC need further study. It is reported that has-miR-142-3p may serve as a prognostic biomarker for ccRCC (Peng *et al.*, 2019). Upregulation of miR-142-3p was correlated with shorter OS and was an independent prognostic factor for ccRCC. Li *et al.* (2016b) found that miR-142-3p significantly suppressed ccRCC cell migration and proliferation, and promoted cell apoptosis. Additionally, has-miR-142-5p has also been shown to promote cervical cancer growth (Hong *et al.*, 2021) and may promote breast cancer resistance to chemotherapy (Wang *et al.*, 2021). Zhu *et al.* (2020a) demonstrated that miR-142-5p targeted TFAP2B and downregulated the expression of TFAP2B, promoting cell proliferation and migration of ccRCC cell lines.

At present, many studies have suggested that has-miR-15b-5p can promote tumor growth of many malignant tumors via various mechanisms (Chen *et al.*, 2018; Dong *et al.*, 2019; Chava *et al.*; 2020; Liu *et al.*, 2020; Miao *et al.*, 2020; Wu *et al.*, 2020; Zhu *et al.*, 2020b; Guo *et al.*, 2021). Most studies (Osanto *et al.*, 2012; Lu *et al.*, 2019; Qi *et al.*, 2020; Cochetti *et al.*, 2022) have shown that has-miR-15b-5p is highly expressed in ccRCC tissues. However, the specific mechanism of has-miR-15b-5p in ccRCC is still unclear. In this study, real-time PCR showed that miR-15b in ccRCC tumor tissue was higher than in normal kidney tissue (P < 0.05). This result is consistent with that by Susanne *et al.* (Osanto *et al.*, 2012), except that Susanne *et al.*, performed whole-genome microRNA sequencing of ccRCC and normal kidney tissues using next-generation deep sequencing technology.

We then explored the clinical significance of miR-15b-5p high expression in ccRCC, and the results showed that the expression level of miR-15b-5p in ccRCC was not significantly correlated with gender, age, smoking history, body mass index, T stage, and pathological nuclear grade. Consistent with the results of this study, Banumathy *et al.*, (Gowrishankar *et al.*, 2014) found no significant difference in the expression of miR-15b-5p in different stages of ccRCC tissues. However, unlike the present study, Banumathy *et al.*, found that miR-15b-5p expression was higher in high-grade ccRCC tissues than in low-grade cancer tissues. Qi *et al.* (2020), found that the expression of miR-15b-5p in ccRCC increased with tumor stage and pathological grade. In this study, bioinformatics analysis indicated that the expression of miR-15b-5p in T1, T2 and M0 phases was lower than that in T3, T4 and M1 phases, respectively. These differences may be caused by different detection methods or sample sizes.

Meanwhile, we studied the relationship between miR-15b-5p and the prognosis of ccRCC patients. Survival analysis showed that within 50 months, patients with high miR-15b-5p expression had shorter DFS; while, after 50 months, patients with high miR-15b-5p expression had longer DFS. However, multivariate analysis showed that upregulation of miR-15b-5p was not a risk factor for disease progression in patients after adjusting for age, sex, smoking history, T stage, and nuclear grade. Additionally, consistent with previous study (Qi *et al.*, 2020), we found through bioinformatics analysis that patients with high expression of miR-15b-5p had shorter OS. At present, most models for the prognosis of ccRCC are based on clinical factors, and there is still a lack of effective biological markers. The results of this study suggest that miR-15b-5p may become a biomarker for the prognosis of ccRCC.

Studies have found that miR-15b-5p has a regulatory effect on the proliferation of prostate cancer, breast cancer, liver cancer, neuroblastoma, lung cancer, cervical cancer, and ovarian cancer (Dong *et al.*, 2019; Chava *et al.*; 2020; Liu *et al.*, 2020; Miao *et al.*, 2020; Wu *et al.*, 2020; Zhu *et al.*, 2020a; Guo *et al.*, 2021). According to our experimental results, down-regulating the expression of miR-15b-5p could inhibit the growth of ccRCC cells, induce apoptosis, and inhibit cell migration and invasion. This is consistent with previous findings (Qi *et al.*, 2020), indicating that miR-15b-5p can promote cell proliferation, invasion and metastasis of ccRCC. Additionally, GO and KEGG analysis in this study showed that the miR-15b-5p target mRNAs were mainly enriched in protein polyubiquitination, protein kinase complex, ubiquitin-like protein transferase activity, P53, and, Progesterone-mediated oocyte maturation. PPI network construction suggested that has-miR-15b-5p-WEE1, has-miR-15b-5p-EIF4E, has-miR-15b-5p-PPP2R1B may be three potential regulatory pathways in ccRCC. However, the results on the role and mechanism of miR-15b-5p in ccRCC are controversial (Osanto *et al.*, 2012; Lu *et al.*, 2019; Qi *et al.*, 2020; Lv *et al.*, 2021; Cochetti *et al.*, 2022). Further studies are warranted.

## CONCLUSION

In conclusion, the expression of miR-15b-5p in ccRCC tissues is higher than that in normal kidney tissues, and it could promote cancer cell proliferation, inhibit cell apoptosis, and promote cancer cell migration and invasion of ccRCC cells. High expression of miR-15b-5p in ccRCC may suggest shorter survival. The has-miR-15b-5p-WEE1, has-miR-15b-5p-EIF4E, and has-miR-15b-5p-PPP2R1B may be three potential regulatory pathways in ccRCC. The tumor-promoting role of miR-15b-5p in ccRCC may make it a new target for the treatment of ccRCC.

**Data availability statement:** This study used the raw data from the GEO database (http://www.ncbi.nlm.nih.govgeo) (including the GSE16441 and GSE189331 datasets) and the TCGA database (https://portal.gdc.cancer.gov/).

**BI, X.; TIAN, M. & CHEN, P.** MiR-15b-5p promueve el crecimiento y la metástasis del carcinoma renal de células claras. *Int. J. Morphol., 41(6)*:1789-1801, 2023.

**RESUMEN:** Investigamos la expresión y la importancia clínica de miR-15b-5p en el carcinoma de células renales (CCR) de células claras mediante análisis bioinformático y verificación experimental. Los miARN expresados diferencialmente se examinaron en la base de datos GEO. El diagrama de Venn mostró que había 5 miARN regulados positivamente (has-miR-210, has-miR-142-3p, has-miR-142-5p, has-miR-15b-5p y has-miR-193a-3p). ) y solo 1 miARN regulado negativamente (has-miR-532-3p) que se expresaron comúnmente entre los conjuntos de datos GSE189331 y GSE16441. Esto fue confirmado aún más en TCGA. Un análisis más detallado mostró que has-miR-193a-3p, has-miR-142-3p, has-miR-142-5p y has-miR-15b-5p estaban estrechamente relacionados con la invasión tumoral, la metástasis a distancia y la probabilidad de supervivencia. La expresión de miR-15b-5p en tejidos ccRCC fue significativamente mayor que la de los tejidos renales normales adyacentes (P <0,05). La expresión de miR-15b-5p no tuvo relación significativa con el sexo, la edad, el historial de tabaquismo, el índice de masa corporal, el estadio T y el grado nuclear patológico (P>0,05). Tras la inhibición de la expresión de miR-15b-5p, las células RCC tuvieron una proliferación atenuada, un aumento de la apoptosis y una migración e invasión atenuadas. has-miR-15b-5p-WEE1, has-miR-15b-5p-EIF4E, has-miR-15b-5p-PPP2R1B pueden ser tres posibles vías reguladoras en ccRCC. miR-15b-5p se expresa altamente en tejidos cancerosos de pacientes con ccRCC. Puede promover la proliferación, inhibir la apoptosis y mejorar la migración celular y la invasión de células RCC. has-miR-15b-5p-WEE1, has-miR-15b-5p-EIF4E y has-miR-15b-5p-PPP2R1B pueden ser tres posibles vías reguladoras en ccRCC.

**PALABRAS CLAVE: MicroARN; Carcinoma de células renales de células claras; PCR en tiempo real; Migración; Análisis bioinformático.**

## REFERENCES

Albiges, L.; Tannir, N.; Burotto, M.; McDermott, D. F.; Plimack, E. R.; Barthélémy, P.; Porta, C. G.; Powles, T. B.; Donskov, F.; George, S.; *et al*. 711P Nivolumab + ipilimumab (N+I) vs sunitinib (S) for first-line treatment of advanced renal cell carcinoma (aRCC) in CheckMate 214: 4-year follow-up and subgroup analysis of patients (pts) without nephrectomy. *Ann. Oncol., 31(Suppl. 4)*:S559-S560, 2020.

Bai, T.; Wang, L.; Wang, D.; Yuan, X.; Bai, W.; Yang, Q. & Yang, X. Clinicopathologica Epidemiological Characteristics and Change Tendencies of Renal Cell Carcinoma in Shanxi Province of China from 2005 to 2014. *PLoS One, 10(12)*:e0144246, 2015.

Bao, J. H.; Li, J. B.; Lin, H. S.; Zhang, W. J.; Guo, B. Y.; Li, J. J.; Fu, L. M. & Sun, Y. P. Deciphering a novel necroptosis-related miRNA signature for predicting the prognosis of clear cell renal carcinoma. *Anal. Cell. Pathol. (Amst.), 2022*:2721005, 2022.

Calin, G. A.; Sevignani, C.; Dumitru, C. D.; Hyslop, T.; Noch, E.; Yendamuri, S.; Shimizu, M.; Rattan, S.; Bullrich, F.; Negrini, M.; *et al*. Human microRNA genes are frequently located at fragile sites and genomic regions involved in cancers. *Proc. Natl. Acad. Sci. U. S. A., 101(9)*:2999-3004, 2004.

Chava, S.; Reynolds, C. P.; Pathania, A. S.; Gorantla, S.; Poluektova, L. Y.; Coulter, D. W.; Gupta, S. C.; Pandey, M. K. & Challagundla, K. B. miR-15a-5p, miR-15b-5p, and miR-16-5p inhibit tumor progression by directly targeting MYCN in neuroblastoma. *Mol. Oncol., 14(1)*:180-96, 2020.

Chen, L. P.; Zhang, N. N.; Ren, X. Q.; He, J. & Li, Y. miR-103/miR-195/miR-15b regulate SALL4 and inhibit proliferation and migration in glioma. *Molecules, 23(11)*:2938, 2018.

Cochetti, G.; Cari, L.; Maulà, V.; Cagnani, R.; Paladini, A.; Del Zingaro, M.; Nocentini, G. & Mearini, E. Validation in an independent cohort of MiR-122, MiR-1271, and MiR-15b as urinary biomarkers for the potential early diagnosis of clear cell renal cell carcinoma. *Cancers (Basel), 14(5)*:1112, 2022.

Dong, Y.; Zhang, N.; Zhao, S.; Chen, X.; Li, F. & Tao, X.  miR-221-3p and miR-15b-5p promote cell proliferation and invasion by targeting Axin2 in liver cancer. *Oncol. Lett., 18(6)*:6491-500, 2019.

Ferlay, J.; Colombet, M.; Soerjomataram, I.; Dyba, T.; Randi, G.; Bettio, M.; Gavin, A.; Visser, O. & Bray, F. Cancer incidence and mortality patterns in Europe: Estimates for 40 countries and 25 major cancers in 2018. *Eur. J. Cancer, 103*:356-87, 2018.

Gowrishankar, B.; Ibragimova, I.; Zhou, Y.; Slifker, M. J.; Devarajan, K.; Al-Saleem, T.; Uzzo, R. G. & Cairns, P. MicroRNA expression signatures of stage, grade, and progression in clear cell RCC. *Cancer Biol. Ther., 15(3)*:329-41, 2014.

Guo, K.; Qi, D. & Huang, B. LncRNA MEG8 promotes NSCLC progression by modulating the miR-15a-5p-miR-15b-5p/PSAT1 axis. *Cancer Cell Int., 21(1)*:84, 2021.

Hong, J. Y.; Zapata, J.; Blackburn, A.; Baumert, R.; Bae, S. M.; Ji, H.; Nam, H. J.; Miller, R. K. & McCrea, P. D. A catenin of the plakophilin-subfamily, Pkp3, responds to canonical-Wnt pathway components and signals. *Biochem. Biophys. Res. Commun., 563*:31-9, 2021.

Ishihara, T.; Seki, N.; Inoguchi, S.; Yoshino, H.; Tatarano, S.; Yamada, Y.; Itesako, T.; Goto, Y.; Nishikawa, R.; Nakagawa, M.; *et al*. Expression of the tumor suppressive miRNA-23b/27b cluster is a good prognostic marker in clear cell renal cell carcinoma. *J. Urol., 192(6)*:1822-30, 2014.

Li, J.; Chen, Y.; Guo, X.; Zhou, L.; Jia, Z.; Tang, Y.; Lin, L.; Liu, W. & Ren, C. Inhibition of miR-15b decreases cell migration and metastasis in colorectal cancer. *Tumour Biol., 37(7)*:8765-73, 2016a.

Li, Y.; Chen, D.; Jin, L. U.; Liu, J.; Li, Y.; Su, Z.; Qi, Z.; Shi, M.; Jiang, Z.; Yang, S.; *et al*. Oncogenic microRNA-142-3p is associated with cellular migration, proliferation and apoptosis in renal cell carcinoma. *Oncol. Lett., 11(2)*:1235-41, 2016b.

Liu, J.; Liu, B.; Guo, Y.; Chen, Z.; Sun, W.; Gao, W.; Wu, H. & Wang, Y. MiR-199a-3p acts as a tumor suppressor in clear cell renal cell carcinoma. *Pathol. Res. Pract., 214(6)*:806-13, 2018.

Liu, L.; Li, Y.; Liu, S.; Duan, Q.; Chen, L.; Wu, T.; Qian, H.; Yang, S. & Xin, D. Downregulation of miR-193a-3p inhibits cell growth and migration in renal cell carcinoma by targeting PTEN. *Tumour Biol., 39(6)*:1010428317711951, 2017.

Liu, Z. J.; Liu, S. H.; Li, J. R.; Bie, X. C. & Zhou, Y. MiR-15b-5b regulates the proliferation of prostate cancer PC-3 cells via targeting LATS2. *Cancer Manag. Res., 12*:10669-78, 2020.

Lu, L.; Li, Y.; Wen, H. & Feng, C. Overexpression of miR-15b promotes resistance to sunitinib in renal cell carcinoma. *J. Cancer, 10(15)*:3389-96, 2019.

Lv, Q.; Wang, G.; Zhang, Y.; Shen, A.; Tang, J.; Sun, Y.; Ma, C. & Wang, P. CircAGAP1 promotes tumor progression by sponging miR-15-5p in clear cell renal cell carcinoma. *J. Exp. Clin. Cancer Res., 40(1)*:76, 2021.

Medina, P. P. & Slack, F. J.  microRNAs and cancer: an overview. *Cell Cycle, 7(16)*:2485-92, 2008.

Miao, S.; Wang, J.; Xuan, L. & Liu, X.  LncRNA TTN-AS1 acts as sponge for miR-15b-5p to regulate FBXW7 expression in ovarian cancer. *Biofactors, 46(4)*:600-7, 2020.

Moch, H.; Cubilla, A. L.; Humphrey, P. A.; Reuter, V. E. and Ulbright, T. M. The 2016 WHO Classification of Tumours of the Urinary System and Male Genital Organs—Part A: Renal, Penile, and Testicular Tumours. *Eur. Urol., 70(1)*:93-105, 2016.

Motzer, R. J.; Escudier, B.; George, S.; Hammers, H. J.; Srinivas, S.; Tykodi, S. S.; Sosman, J. A.; Plimack, E. R.; Procopio, G.; McDermott, D. F.; *et al*. Nivolumab versus everolimus in patients with advanced renal cell carcinoma: Updated results with long-term follow-up of the randomized, open-label, phase 3 CheckMate 025 trial. *Cancer, 126(18)*:4156-67, 2020.

Motzer, R.; Jonasch, E.; Michaelson, M.; Nandagopal, L.; Gore, J. L.; George, S.; Alva, A.; Haas, N.; Harrison, M. R.; Plimack, E. R.; *et al*. NCCN Guidelines Insights: Kidney Cancer, Version 2.2020. *J. Natl. Compr. Canc. Netw., 17(11)*:1278-85, 2019.

Osanto, S.; Qin, Y.; Buermans, H. P.; Berkers, J.; Lerut, E.; Goeman, J. J. & van Poppel, H. Genome-wide microRNA expression analysis of clear cell renal cell carcinoma by next generation deep sequencing. *PLoS One, 7(6)*:e38298, 2012.

Pang, C.; Guan, Y.; Zhao, K.; Chen, L.; Bao, Y.; Cui, R.; Li, G. & Wang, Y. Up-regulation of microRNA-15b correlates with unfavorable prognosis and malignant progression of human glioma. *Int. J. Clin. Exp. Pathol., 8(5)*:4943-52, 2015.

Peng, X.; Pan, X.; Liu, K.; Zhang, C.; Zhao, L.; Li, H.; Guan, X.; Xu, W.; Xu, J.; Zhang, F.; *et al*. miR-142-3p as a novel biomarker for predicting poor prognosis in renal cell carcinoma patients after surgery. *Int. J. Biol. Markers, 34(3)*:302-8, 2019.

Qi, Y.; Ma, Y.; Peng, Z.; Wang, L.; Li, L.; Tang, Y.; He, J. & Zheng, J. Long noncoding RNA PENG upregulates PDZK1 expression by sponging miR-15b to suppress clear cell renal cell carcinoma cell proliferation. *Oncogene, 39(22)*:4404-20, 2020.

Skolarikos, A.; Alivizatos, G.; Laguna, P. & de la Rosette, J. A review on follow-up strategies for renal cell carcinoma after nephrectomy. *Eur. Urol., 51(6)*:1490-500; discussion 501, 2007.

Spyropoulou, D.; Tsiganos, P.; Dimitrakopoulos, F. I.; Tolia, M.; Koutras, A.; Velissaris, D.; Lagadinou, M.; Papathanasiou, N.; Gkantaifi, A.; Kalofonos, H.; *et al*. Radiotherapy and renalcell carcinoma: a continuing saga. *In Vivo, 35(3)*:1365-77, 2021.

Wang, L.; Zhou, Y.; Jiang, L.; Lu, L.; Dai, T.; Li, A.; Chen, Y. & Zhang, L. CircWAC induces chemotherapeutic resistance in triple-negative breast cancer by targeting miR-142, upregulating WWP1 and activating the PI3K/AKT pathway. *Mol. Cancer, 20(1)*:43, 2021.

Wang, S. S.; Huang, Z. G.; Wu, H. Y.; He, R. Q.; Yang, L. H.; Feng, Z. B.; Dang, Y. W.; Lu, H. P.; Fang, Y. Y. & Chen, G. Downregulation of miR-193a-3p is involved in the pathogenesis of hepatocellular carcinoma by targeting CCND1. *PeerJ, 8*:e8409, 2020.

Wen, H.; Fu, Y.; Zhu, Y.; Tao, S.; Shang, X.; Li, Z.; You, T. & Zhang, W. Long non-coding RNA KRT8P41/miR-193a-3p/FUBP1 axis modulates the proliferation and invasion of chordoma cells. *J. Bone Oncol., 31*:100392, 2021.

Wu, B.; Liu, G.; Jin, Y.; Yang, T.; Zhang, D.; Ding, L.; Zhou, F.; Pan, Y. & Wei, Y. miR-15b-5p promotes growth and metastasis in breast cancer by targeting HPSE2. *Front. Oncol., 10*:108, 2020.

Zhang, Y.; Huang, F.; Wang, J.; Peng, L. & Luo, H. MiR-15b mediates liver cancer cells proliferation through targeting BCL-2. *Int. J. Clin. Exp. Pathol., 8(12)*:15677-83, 2015.

Zhu, M.; Zou, L.; Lu, F.; Ye, L.; Su, B.; Yang, K.; Lin, M.; Fu, J. & Li, Y. miR-142-5p promotes renal cell tumorigenesis by targeting TFAP2B. *Oncol. Lett., 20(6)*:324, 2020a.

Zhu, Y.; Zhang, X.; Wang, L.; Zhu, X.; Xia, Z.; Xu, L. & Xu, J. FENDRR suppresses cervical cancer proliferation and invasion by targeting miR-15a/b-5p and regulating TUBA1A expression. *Cancer Cell Int., 20*:152, 2020b.

Corresponding author:
Peng Chen
Department of Urology
Affiliated Tumor Hospital of Xinjiang Medical University
No. 789, Suzhou East Street
Xinshi District
Urumqi
CHINA

E-mail: Xjchenpeng1@163.com